



THE UNIVERSITY *of* EDINBURGH

## Edinburgh Research Explorer

### Imaging Proteins Sensitive to Direct Fusions Using Transient Peptide–Peptide Interactions

**Citation for published version:**

Gidden, Z, Oi, C, Johnston, EJ, Konieczna, Z, Bhaskar, H, Mendive-Tapia, L, De moliner, F, Rosser, SJ, Mochrie, SGJ, Vendrell, M, Horrocks, MH & Regan, L 2023, 'Imaging Proteins Sensitive to Direct Fusions Using Transient Peptide–Peptide Interactions', *Nano Letters*, vol. 23, no. 22, pp. 10633-10641. <https://doi.org/10.1021/acs.nanolett.3c03780>

**Digital Object Identifier (DOI):**

[10.1021/acs.nanolett.3c03780](https://doi.org/10.1021/acs.nanolett.3c03780)

**Link:**

[Link to publication record in Edinburgh Research Explorer](#)

**Document Version:**

Publisher's PDF, also known as Version of record

**Published In:**

Nano Letters

**Publisher Rights Statement:**

This article is licensed under CC-BY-4.0. Open Access.

**General rights**

Copyright for the publications made accessible via the Edinburgh Research Explorer is retained by the author(s) and / or other copyright owners and it is a condition of accessing these publications that users recognise and abide by the legal requirements associated with these rights.

**Take down policy**

The University of Edinburgh has made every reasonable effort to ensure that Edinburgh Research Explorer content complies with UK legislation. If you believe that the public display of this file breaches copyright please contact [openaccess@ed.ac.uk](mailto:openaccess@ed.ac.uk) providing details, and we will remove access to the work immediately and investigate your claim.



# Imaging Proteins Sensitive to Direct Fusions Using Transient Peptide–Peptide Interactions

Zoe Gidden,<sup>□</sup> Curran Oi,<sup>□</sup> Emily J. Johnston, Zuzanna Konieczna, Haresh Bhaskar, Lorena Mendive-Tapia, Fabio de Moliner, Susan J. Rosser, Simon G. J. Mochrie, Marc Vendrell, Mathew H. Horrocks,\* and Lynne Regan\*



Cite This: *Nano Lett.* 2023, 23, 10633–10641



Read Online

ACCESS |

Metrics & More

Article Recommendations

Supporting Information

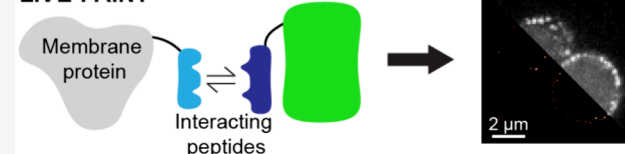
**ABSTRACT:** Fluorescence microscopy enables specific visualization of proteins in living cells and has played an important role in our understanding of the protein subcellular location and function. Some proteins, however, show altered localization or function when labeled using direct fusions to fluorescent proteins, making them difficult to study in live cells. Additionally, the resolution of fluorescence microscopy is limited to  $\sim 200$  nm, which is 2 orders of magnitude larger than the size of most proteins. To circumvent these challenges, we previously developed LIVE-PAINT, a live-cell super-resolution approach that takes advantage of short interacting peptides to transiently bind a fluorescent protein to the protein-of-interest. Here, we successfully use LIVE-PAINT to image yeast membrane proteins that do not tolerate the direct fusion of a fluorescent protein by using peptide tags as short as 5-residues. We also demonstrate that it is possible to resolve multiple proteins at the nanoscale concurrently using orthogonal peptide interaction pairs.

**KEYWORDS:** *membrane protein, protein–protein interaction, super-resolution microscopy, live-cell imaging, LIVE-PAINT, yeast*

## Direct fusion



## LIVE-PAINT



The ability to visualize proteins in their native cellular environment using direct genetic fusion to a fluorescent protein (FP) has revolutionized cell biology. Unfortunately, not all proteins tolerate fusion to a FP, and can mislocalize or malfunction.<sup>1,2</sup> One class of proteins that are frequently perturbed are yeast membrane transporter proteins, which show little or no localization to the plasma membrane when green fluorescent protein (GFP) is directly fused to their C-terminus.<sup>3,4</sup> The highly abundant proton pump Pma1, for example, is well-known to localize to the plasma membrane; however, Pma1 tagged with GFP at the C-terminus primarily localizes to the vacuole.<sup>3,4</sup> Another easily perturbed protein in yeast is the nicotinic acid transporter Tna1, which is retained in the endoplasmic reticulum rather than localizing to the plasma membrane when tagged at the C-terminus with GFP.<sup>9</sup>

Imaging protein subcellular localization using fusions to FPs or other fluorescence techniques also has the drawback that the resolution is restricted to  $\sim 200$  nm due to the diffraction of light, unless a super-resolution (SR) technique is used.<sup>10–12</sup> SR microscopy is an umbrella term for techniques that either illuminate a region of the sample smaller than the diffraction limit or use stochastic activation of fluorophores to enable the identification and precise localization of single emitters.<sup>13</sup> Most SR techniques are challenging to apply to live-cell imaging, however, stimulated emission depletion (STED),<sup>11</sup> reversible

saturable optical fluorescence transition (RESOLFT);<sup>14</sup> structured illumination microscopy (SIM);<sup>15</sup> and some single-molecule localization microscopy (SMLM) approaches, such as photoactivated localization microscopy (PALM),<sup>10</sup> have been used to obtain SR images of proteins in live cells. For a comprehensive overview of live-cell SR techniques, see Godin, Lounis, and Cognet, 2014.<sup>16</sup>

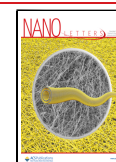
Furthermore, SR imaging of more than two proteins in live cells remains challenging unless SIM is used, but the improvement in resolution relative to diffraction limited imaging is only around 2-fold.<sup>17</sup> Halo,<sup>18</sup> SNAP,<sup>19</sup> and CLIP<sup>20</sup> are orthogonal protein tags can be used to label proteins with exogenously added fluorescently labeled ligands and have been used for two-color SR microscopy in living cells.<sup>21–23</sup> Three color SR imaging has been achieved in live cells by combining PALM with direct stochastic optical reconstruction microscopy (dSTORM).<sup>24</sup> However, both of

**Received:** October 3, 2023

**Revised:** October 30, 2023

**Accepted:** October 30, 2023

**Published:** November 2, 2023



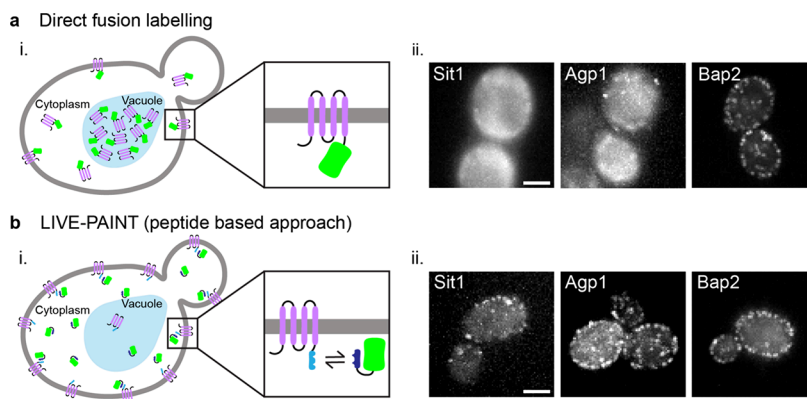


**Figure 1.** Membrane transporter proteins tolerate peptide fusions better than direct fusion to a FP. (ai) Membrane protein (purple) directly fused to a FP (green) often mislocalizes to the vacuole (light blue oblong shape) or cytoplasm rather than locating to the plasma membrane (gray). (aii) Diffraction-limited TIRF images of three different membrane transporter proteins labeled by directly fusing mNG to their C-terminus. Scale bar is 2  $\mu\text{m}$  and all images have the same dimensions. (bi) Membrane proteins fused to one-half of a coiled-coil peptide (light blue rod) are less likely to mislocalize and can be imaged using the other half of the coiled-coil peptide (dark blue rod) fused to a FP. (bii) Diffraction-limited TIRF images the same three membrane transporter proteins tagged using the 101A/101B coiled coil pair: one-half is fused to the C-terminus of the membrane protein, and the other half is fused to mNG and expressed *in vivo*. Scale bar is 2  $\mu\text{m}$  and all images have the same dimensions.

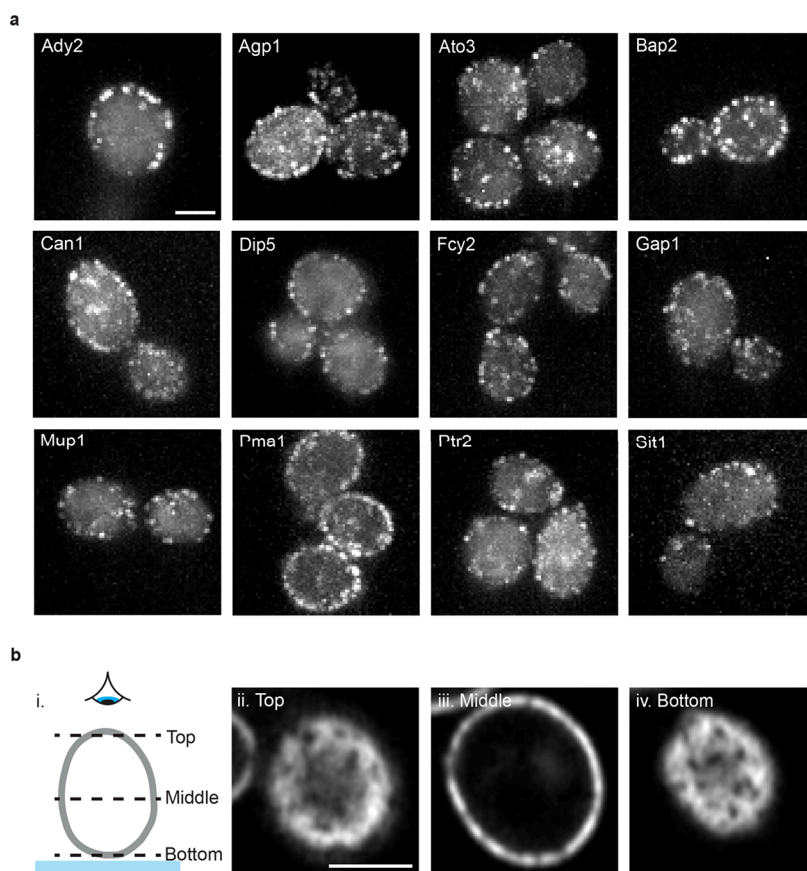


**Figure 2.** Membrane proteins imaged using the peptide tagging approach show a fluorescent signal at the plasma membrane in live cells. (a) Diffraction-limited TIRF images of membrane transporter proteins tagged with the 101B peptide at their C-terminus and imaged by coexpressing 101A-mNG. Scale bar is 2  $\mu\text{m}$  and all images have the same dimensions. (bi) Schematic representation of z slices through a yeast cell shown in (bii)–(biv). Glass slide represented by the blue band and an eye showing the view from above. (bii–biv) Top, middle, and bottom z slices of Pma1–101B imaged by coexpressing 101A-mNG acquired using an Airyscan microscope. Scale bar in part bii is 2  $\mu\text{m}$  and all images bii–biv have the same dimensions.

these multicolor strategies and most other live-cell SR techniques use FPs ( $\sim 25$  kDa) or large protein tags (33 kDa for HaloTag and  $\sim 20$  kDa for SNAP-tag and CLIP-tag) to label the protein being studied, which can be detrimental to normal localization and function. Peptide based point

accumulation for imaging in nanoscale topography (PAINT) approaches offer a solution to the large tags often necessary for live-cell SR microscopy but have so far only been used to image proteins on the surface of live cells or to image internal structures in fixed cells.<sup>25–27</sup>

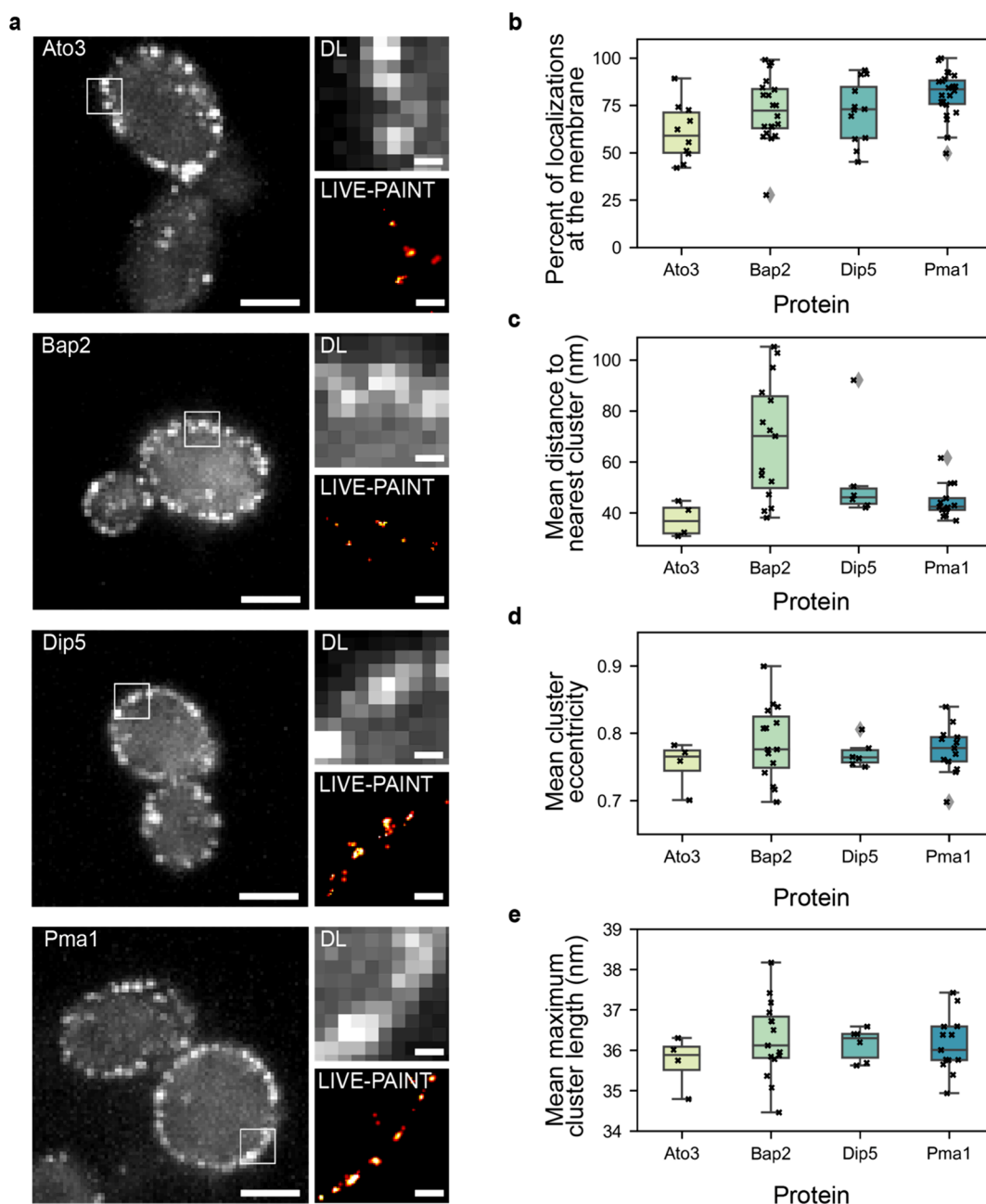


**Figure 3.** Live cell imaging of membrane proteins using LIVE-PAINT measures protein localization with nanometer precision. (a) Diffraction-limited and super-resolution LIVE-PAINT images for four representative membrane transporter proteins; Ato3, Bap2, Dip5, and Pma1. For these proteins, 101B is fused to the C-terminus and imaged by coexpressing 101A-mNG. Scale bars are 2  $\mu\text{m}$  for full-cell images and 250 nm for zoom ins. Full-cell LIVE-PAINT images are shown in Figure S5. (b–e) Box plots showing the mean value for (b) percent of localizations at the membrane, (c) distance to the nearest cluster, (d) cluster eccentricity, and (e) maximum cluster length for each cell imaged. Ato3 ( $n = 4$  cells), Bap2 ( $n = 15$  cells), Dip5 ( $n = 6$  cells), and Pma1 ( $n = 13$  cells).

We have recently developed a live-cell SR imaging method that can be applied to proteins that do not tolerate a direct fusion to a FP. Rather than directly fusing the protein-of-interest to a FP, Live cell Imaging using reVersible intERactions Point Accumulation for Imaging in Nanoscale Topography (LIVE-PAINT) uses noncovalent transient interactions between a peptide fused to the target protein, and the binding partner of the peptide fused to a FP.<sup>28</sup> The use of the small peptide tag (<5 kDa) renders this approach less perturbative than direct FP fusions. Here, we demonstrate that LIVE-PAINT can be used to locate a variety of difficult-to-image membrane proteins in yeast with nanometer precision. For

proteins that are particularly sensitive to modifications, we show that it is possible to implement LIVE-PAINT on proteins tagged with only a 5-residue peptide (<1 kDa).

Furthermore, using multiple orthogonal peptide–peptide interaction pairs and FPs with different emission wavelengths, we image two membrane-associated proteins simultaneously with nanometer precision. Although we demonstrate this functionality using membrane-associated proteins here, we expect that LIVE-PAINT will enable us to visualize any difficult-to-label protein at the nanometer length scale. Additionally, LIVE-PAINT can be performed using any bright FP, unlike PALM, which requires photoactivatable or photo-

convertible FPs.<sup>12</sup> This means that LIVE-PAINT has access to a much larger array of FPs, with varied absorption and emission spectra; this makes LIVE-PAINT an ideal SR method for tagging and imaging multiple target proteins concurrently.

### ■ SMALL PEPTIDE TAGS ENABLE VISUALIZATION OF FUSION-SENSITIVE MEMBRANE PROTEINS

Rather than relying on the genetically encoded fusion of full-length FPs to target proteins, LIVE-PAINT uses a peptide–peptide interaction pair to noncovalently and transiently associate a FP with the protein-of-interest (Figure 1ai,bi). We hypothesized that the fusion of a small peptide tag to the target protein would be less perturbative to the localization or function of the protein than direct fusion to a FP, and we therefore sought to apply LIVE-PAINT to image membrane proteins that mislocalize or have proven difficult to visualize when directly fused to GFP.

We first selected a set of *Saccharomyces cerevisiae* membrane transporter proteins that either accumulate at the vacuole or cannot be visualized upon direct fusion to GFP.<sup>4</sup> Other researchers have previously carried out diffraction limited imaging of membrane proteins by labeling the target protein with a coiled-coil oriented outside of the cell and introducing the partner peptide in the imaging buffer so we anticipated our LIVE-PAINT approach would be feasible.<sup>29</sup> We fused the coiled-coil peptide 101B to the C-terminus of each of these membrane proteins; the C-terminus for each of these proteins is predicted to be cytoplasmic.<sup>30</sup> We also integrated a gene encoding the coiled-coil peptide 101A fused to mNeonGreen (mNG) into the genome driven by the galactose-inducible promoter pGAL1,<sup>28</sup> replacing the *GAL2* gene in the process. Chen et al. designed the 101A/101B leucine zipper coiled-coils and showed that they interact with an estimated  $K_d$  of  $\sim 200$  nM in the cytosol of live yeast.<sup>31</sup>

When imaged using total internal reflection fluorescence (TIRF) microscopy, membrane proteins tagged using the LIVE-PAINT system appear as a ring around the periphery of the cell (Figure 1bii). However, this does depend on the orientation of the yeast on the slide, the TIR angle, and the  $z$  plane used for imaging.

We subsequently used LIVE-PAINT to image a collection of 12 plasma membrane proteins that have been reported to exhibit partial or complete mislocalization when directly fused to GFP in yeast (Figure 2a).<sup>4</sup> For the negative control, 101A-mNG expressed in yeast in the absence of a target protein fused to 101B, we did not observe more than background fluorescence at any specific location within the cell, including at the plasma membrane (Figure S4). In addition, we demonstrate that the function of the protein is not impaired by tagging with 101B for LIVE-PAINT imaging for three of these strains (Figures S2 and S3). We found that the success of this approach does not depend on the abundance of the membrane protein, although there is generally improved contrast between the membrane signal and background signal for more abundant proteins (see Table S1 for approximate abundance and Figure 2a). We believe that this effect is because the fraction of FP bound to the target protein should increase as the concentration of target protein increases.

To demonstrate that this technique was compatible with other widely available microscopy techniques, we used LIVE-PAINT to image Pma1 in different planes through the yeast cell using a Zeiss LSM880 confocal microscope with Airyscan (Figure 2b). This also enabled a 3D rendering of the

distribution of Pma1 throughout the entire cell (Video S1). Clear plasma membrane signal with minimal internal signal is observed in the plane that cuts through the middle of the cell (Figure 2biii). In both planes that cut through the membrane at the top and bottom of the cell, regions where Pma1 is excluded can be clearly observed (Figures 2bii and 2biv). This is consistent with the network-like distribution, exclusive of the membrane compartment of Can1 domains or eisosomes, which has previously been described for Pma1. This is expected as Pma1 is known to be arranged in microcompartments at the membrane.<sup>32</sup>

### ■ SUPER-RESOLUTION IMAGING OF MEMBRANE PROTEINS REVEALS CLOSELY SPACED PROTEIN CLUSTERS

We next selected four membrane transporter proteins that showed clear localization at the plasma membrane when tagged using 101A/101B for super-resolution imaging using LIVE-PAINT (Figure 3a). In less than two min of data acquisition for Pma1, LIVE-PAINT led to  $367 \pm 315$  localizations (mean  $\pm$  SD,  $n = 15$  cells) with a precision of  $10.7 \pm 0.4$  nm (mean  $\pm$  SD,  $n = 15$  cells), leading to a resolution of  $67.3 \pm 13.4$  nm (mean  $\pm$  SD,  $n = 15$  cells) (calculated using Fourier Ring Correlation (10 Brink, T. RustFRC [Computer software]) (see Table S2 for a summary of resolution, precision, and number of localizations achieved for each protein presented in Figure 3). Although not our focus in this work, it is possible to extend the imaging time beyond 2 min to obtain a higher number of localizations (Figure S9).<sup>28</sup>

The success of the labeling strategy was measured by quantifying the percentage of localizations at the membrane (Figure 3b). We found that 60%, 70%, 67%, and 82% of total localizations were at the membrane for Ato3, Bap2, Dip5, and Pma1, respectively. The resulting images revealed clusters of localizations spaced less than 200 nm apart (Figures 3c and S6a). We were also able to measure the eccentricity (Figures 3d and S6b) and maximum cluster length (Figure 3e and S6c) for the clusters detected. We found that most of the clusters were elliptical, with eccentricity values close to 1, which is expected, as they are bounded in one axis by the width of the membrane. These protein clusters are too small, approximately 36 nm in length, and are spaced too close to one another to be distinguished by diffraction-limited microscopy. This highlights the importance of imaging such proteins using SR methods, as such detailed information about their arrangement would not be possible to measure with other techniques.

### ■ A FIVE-RESIDUE FUSION TAG IS SUFFICIENT TO ENABLE LIVE-CELL SUPER-RESOLUTION IMAGING

Although most proteins will tolerate fusion to a 5 kDa peptide tag, sometimes this may be too large, and we therefore sought to demonstrate LIVE-PAINT with a shorter peptide tag. For this purpose, we selected the 5-residue KQTSV peptide that binds reversibly to the 11 kDa protein PDZ3. To test this system, we fused KQTSV to the endogenous septum protein Cdc12 and coexpressed PDZ3 protein fused to mNG under the galactose inducible promoter (Figure S11). While it was possible to observe some fluorescence at the septum (diffraction-limited and LIVE-PAINT images shown in Figure S11b), there was also significant background fluorescence in the cell, and the spatial resolution was lower than expected ( $269 \pm 108$  nm, mean  $\pm$  SD,  $n = 5$  cells). We reasoned that

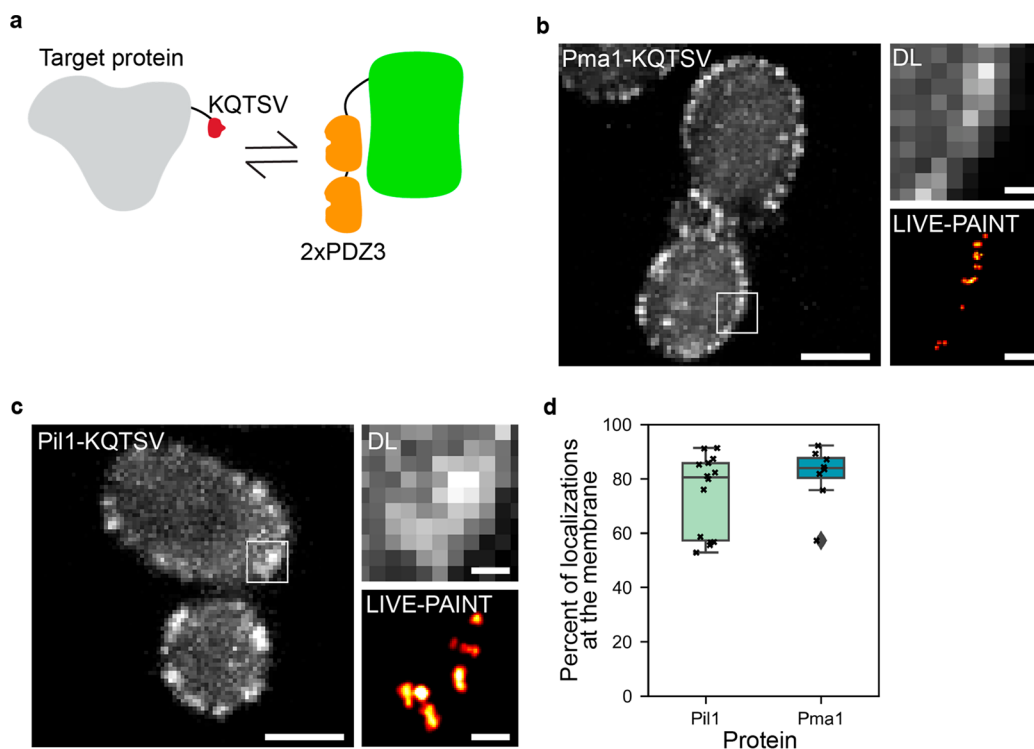


**Figure 4.** The 5-residue tag KQTSV can be used for LIVE-PAINT imaging of membrane proteins in live cells. (a) Schematic representation of the labeling strategy. The short KQTSV peptide (red) is used to label the target protein, and this reversibly binds to the 2xPDZ3 protein (orange units), which are attached to mNG. (b, c) Diffraction-limited (DL) and super-resolution LIVE-PAINT images for two membrane associated proteins. For these proteins, KQTSV is fused to the C-terminus and imaged by coexpressing 2xPDZ3-mNG. Scale bars are 2  $\mu\text{m}$  for full-cell images and 250 nm for zoom ins. Full-cell LIVE-PAINT images are shown in Figure S13. (d) Box plots showing the percentage of total localizations at the membranes for Pil1 and Pma1.

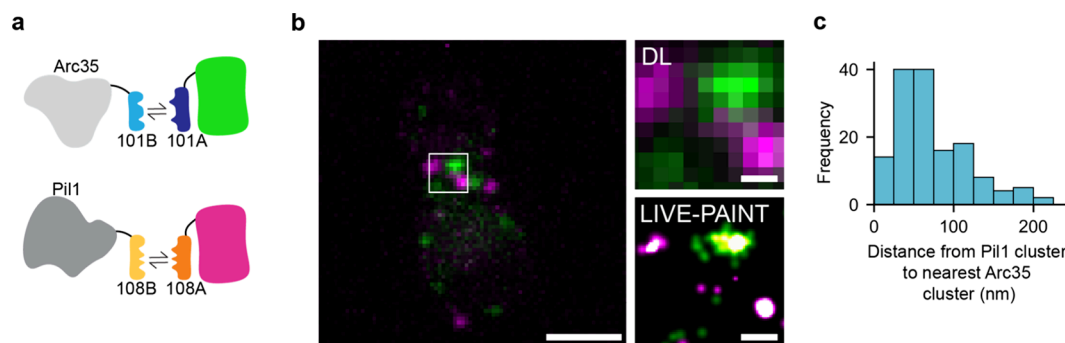


**Figure 5.** LIVE-PAINT can be used to image two proteins in live cells, concurrently, with nanometer precision. (a) Schematic representation of the LIVE-PAINT labeling strategy used to image Arc35 and Pil1 simultaneously. The orthogonal peptide pairs 101A/101B and 108A/108B were used to label Arc35 and Pil1 with mNG and mCherry, respectively. (b) Diffraction-limited and SR images of Arc35 (green) and Pil1 (magenta) simultaneously imaged using the LIVE-PAINT. Scale bars are 2  $\mu\text{m}$  for full-cell images and 250 nm for zoom ins. (c) Histogram showing the distance between each Pil1 cluster and its closest Arc35 cluster in the same cell ( $n = 6$  cells).

this was due to the low affinity of the KQTSV/PDZ3 system ( $K_D$  670  $\pm$  110 nM, mean  $\pm$  SD,  $n = 2$ , see Figure S12),<sup>33</sup> and we therefore trialed tagging mNG with two tandem repeats of the PDZ3 protein, in an approach analogous to that utilized with DNA-PAINT to enhance the signal-to-background ratio.<sup>34</sup> It is worth noting that this approach does not change the  $K_D$ , we measured the  $K_D$  for the KQTSV/2xPDZ3 system to be the same as the 1xPDZ system (680  $\pm$  170 nM, mean  $\pm$  SD,  $n = 3$ , see Figure S12). As expected, this led to clearer images of the septum (Figure S11b), and a higher resolution was obtained (123  $\pm$  37 nm, mean  $\pm$  SD,  $n = 14$  cells) (imaging of Cdc12 using 101A/B and the negative control with 2xPDZ3 only is also shown in Figure S11).

After establishing the feasibility of using the 2xPDZ3/KQTSV protein-peptide pair for LIVE-PAINT imaging, we used this interaction pair to image two more proteins: Pma1, which is not amenable to direct fusions to GFP, and Pil1, which is a membrane-associated protein (Figure 4). Similar to the 101A/B peptide pair, imaging using the 2xPDZ3/KQTSV interaction pair produces clear plasma membrane localizations for both Pma1 and Pil1 with very little internal signal for both the diffraction-limited and SR images (Figure 4b,c). To quantify the success of the labeling strategy, the percentage of the membrane specific to total localizations was calculated for each protein (Figure 4d). On average, for Pma1, 83% of localizations were at the membrane and for Pil1 74% of

localizations were membrane specific. See Table S3 for a summary of the resolution, precision, and number of localizations achieved for Pma1 and Pil1 imaged with the 2xPDZ3/KQTSV protein-peptide pair. The success of this labeling approach demonstrates the generalizability of LIVE-PAINT: other interaction pairs, not only 101A/101B, can be used to achieve clear labeling of membrane proteins that mislocalize when directly fused to GFP.

### ■ LIVE-PAINT ENABLES SIMULTANEOUS LIVE-CELL SUPER-RESOLUTION IMAGING OF TWO PROTEINS

As two-color live-cell SR imaging is challenging with current methods and often requires a direct fusion to an FP, we sought to use LIVE-PAINT to image two proteins simultaneously in live cells. We chose to image two plasma membrane associated proteins, Arc35 and Pil1, which are predicted to be close together but not localized to the same structures. Arc35 is a component of actin patches and assists in the organization of actin to facilitate endocytosis<sup>35</sup> and Pil1 is a BAR domain protein that facilitates the formation of eisosome subdomains of the plasma membrane,<sup>36</sup> which are associated with sites of protection from endocytosis.<sup>37</sup> We used two leucine zipper coiled-coils, 101A/101B and 108A/108B, that have previously been shown to be orthogonal,<sup>31</sup> to C-terminally tag Arc35 and Pil1, respectively (Figure 5a).<sup>31</sup> 101A fused to mNG was integrated into the genome and expressed under the galactose inducible promoter, pGAL1, as before, and 108A fused to mCherry was also integrated into the genome and expressed under the same promoter.

The SR images generated show that Arc35 and Pil1 are arranged in clusters with little to no overlap between the two proteins (Figure 5b). We achieved a resolution of  $83 \pm 22$  nm (mean  $\pm$  SD,  $n = 6$  cells) with mNG and  $68 \pm 24$  nm (mean  $\pm$  SD,  $n = 6$  cells) with mCherry (10 Brink, T. RustFRC [Computer software]) (see Table S4 for a summary of resolution, precision and number of localizations achieved for Arc35 and Pil1 in Figure 5). For each Pil1 cluster, we calculated the distance to the nearest Arc35 cluster (Figure 5c) and found that all of the nearest clusters were closer than the diffraction-limit of light (210 nm), meaning that they would not be spatially distinguished using standard fluorescence microscopy. This demonstrates the value of using a live-cell SR imaging technique for concurrent imaging of proteins such as Arc35 and Pil1 that localize near each other in the cell.

### ■ CONCLUSIONS AND DISCUSSION

We have demonstrated that proteins sensitive to direct fusion to GFP can be fused to a small peptide and imaged in live cells using the binding partner of the peptide fused to a FP. We used membrane transporter proteins as an example class of proteins that are generally sensitive to direct fusion to GFP and show that they generally tolerate fusion to a small (<5 kDa) peptide and subsequent LIVE-PAINT imaging. Our approach clearly recovers the expected localization of the tagged protein in 12 membrane transporter proteins we tagged and imaged. We also carried out 3D imaging on one of the membrane proteins, Pma1, using a peptide tagging approach. Additionally, we have also demonstrated that we can perform LIVE-PAINT SR imaging of multiple proteins in yeast, both separately and simultaneously using two orthogonal peptide-peptide interaction pairs.

We expect this approach to be broadly useful for tagging and imaging proteins sensitive to direct fusions to a FP. Here, we have demonstrated the use of LIVE-PAINT for imaging yeast membrane transporter proteins, but the small size of the peptides used relative to a FP suggests that this approach will be useful for visualizing other difficult-to-label proteins.<sup>4,38,39</sup> We note that while we successfully used LIVE-PAINT to image membrane proteins with a variety of abundances, we generally found that higher abundance proteins produced images with a clearer membrane signal. In our previous work, we have shown that, like other PAINT-based methods, LIVE-PAINT enables long imaging times through replenishment of imaging strands.<sup>28,40</sup> For low abundance proteins, it may be beneficial to extend imaging times to obtain a higher number of total localizations.

In addition to showing that our peptide tagging approach can be less perturbative to the localization of the target protein, we showed that the binding affinity of the interaction of peptide-peptide or peptide-protein pairs was important for successful LIVE-PAINT imaging. Through this work and our previous work, we have found that interaction pairs with a binding affinity between 1 and 300 nM work well;<sup>28</sup> however, here we also show that weaker binding pairs can potentially be used if the number of binding sites available on the imaging strand is increased. For proteins that do not tolerate a 5-residue-tag it is also possible to use the imaging strand to directly label the protein target in a technique called direct-LIVE-PAINT.<sup>41</sup> However, this approach is less universal than LIVE-PAINT as it relies on the generation or presence of existing peptide probes that bind directly to the endogenous target protein with appropriate kinetics for LIVE-PAINT.

Finally, we demonstrate that LIVE-PAINT can be used to image two targets simultaneously in live cells. This approach could be used to carry out live-cell colocalization studies on proteins that do not tolerate direct fusions and to investigate colocalization at resolutions higher than the diffraction-limit of light. Two-color imaging using E/K coiled-coil interaction pairs has also been demonstrated by Eklund and Jungmann in fixed mammalian cells.<sup>42</sup> To date, we have used 5 different interaction pairs for LIVE-PAINT imaging: the protein-peptide interaction pairs TRAP4/MEEVF and 2xPDZ3/KQTSV, and the peptide-peptide interaction pairs SYNZIP17/SYNZIP18, 101A/B and 108A/B.<sup>28</sup> The diversity of interaction pairs suitable for LIVE-PAINT illustrates the broad potential of this approach for tagging and imaging proteins sensitive to direct fusions to FPs. Similarly, the growing set of orthogonal interaction pairs that we have shown to be suitable for LIVE-PAINT reveals the potential for simultaneous live-cell SR imaging of multiple proteins; here, we demonstrate this with two proteins, but we envision that simultaneous LIVE-PAINT imaging of three or more proteins is also possible.

### ■ ASSOCIATED CONTENT

#### SI Supporting Information

The Supporting Information is available free of charge at <https://pubs.acs.org/doi/10.1021/acs.nanolett.3c03780>.

Movie of a 3D rendering of Pma1 labeled using LIVE-PAINT (Video S1) (AVI)

Materials and methods; representative crystal structures of the interacting peptide pairs used in this study (Figure S1); cell growth analysis to show that function is not impaired by tagging with a peptide for LIVE-PAINT

(Figures S2 and S3); negative control for LIVE-PAINT imaging with 101A-mNeonGreen and 2xPDZ3-mNeonGreen (Figures S4 and S11, respectively); comparison of LIVE-PAINT imaging with 101A, 1xPDZ3, or 2xPDZ3 fused to mNeonGreen (Figure S11); full-cell super-resolution images of proteins imaged using LIVE-PAINT (Figure S5 and S13); supporting analysis of protein clusters (Figures S6 and S7); histograms of photon counts for images presented in Figure 3 (Figure S8); representative plots to show localization classification as membrane, cellular or external (Figures S10 and S14); quantification of localizations detected during LIVE-PAINT imaging (Figure S9); graphs of diffusion lag time used to measure the binding kinetics of 1xPDZ3 and 2xPDZ3 with the KQTSV peptide (Figure S12); list of proteins imaged in this study (Table S1); summary statistics for all super-resolution images (Tables S2–S4); constructs used to measure the binding kinetics of the PDZ peptides (Table S5); list of primers used in this study (Tables S6 and S7); and list of yeast strains used in this study (Table S8) (PDF)

## AUTHOR INFORMATION

### Corresponding Authors

**Lynne Regan** – School of Biological Sciences, University of Edinburgh, Edinburgh EH9 3DW, U.K.; Centre for Engineering Biology, University of Edinburgh, Edinburgh EH9 3BF, U.K.; Integrated Graduate Program in Physical and Engineering Biology, Yale University, New Haven, Connecticut 06520, United States; Institute of Quantitative Biology, Biochemistry and Biotechnology, Edinburgh EH9 3FF, U.K.; Email: [lynne.regan@ed.ac.uk](mailto:lynne.regan@ed.ac.uk)

**Mathew H. Horrocks** – EaStCHEM School of Chemistry, The University of Edinburgh, Edinburgh EH9 3FJ, U.K.; IRR Chemistry Hub, Institute for Regeneration and Repair, The University of Edinburgh, Edinburgh EH16 4UU, U.K.; [orcid.org/0000-0001-5495-5492](https://orcid.org/0000-0001-5495-5492); Email: [mathew.horrocks@ed.ac.uk](mailto:mathew.horrocks@ed.ac.uk)

### Authors

**Zoe Gidden** – School of Biological Sciences, University of Edinburgh, Edinburgh EH9 3DW, U.K.; EaStCHEM School of Chemistry, The University of Edinburgh, Edinburgh EH9 3FJ, U.K.

**Curran Oi** – Department of Genome Sciences, University of Washington, Seattle, Washington 98195, United States

**Emily J. Johnston** – School of Biological Sciences, University of Edinburgh, Edinburgh EH9 3DW, U.K.; Centre for Engineering Biology, University of Edinburgh, Edinburgh EH9 3BF, U.K.

**Zuzanna Konieczna** – EaStCHEM School of Chemistry, The University of Edinburgh, Edinburgh EH9 3FJ, U.K.; IRR Chemistry Hub, Institute for Regeneration and Repair, The University of Edinburgh, Edinburgh EH16 4UU, U.K.

**Haresh Bhaskar** – School of Biological Sciences, University of Edinburgh, Edinburgh EH9 3DW, U.K.; EaStCHEM School of Chemistry, The University of Edinburgh, Edinburgh EH9 3FJ, U.K.; IRR Chemistry Hub, Institute for Regeneration and Repair, The University of Edinburgh, Edinburgh EH16 4UU, U.K.

**Lorena Mendive-Tapia** – IRR Chemistry Hub, Institute for Regeneration and Repair and Centre for Inflammation

Research, The University of Edinburgh, Edinburgh EH16 4UU, U.K.

**Fabio de Moliner** – IRR Chemistry Hub, Institute for Regeneration and Repair and Centre for Inflammation Research, The University of Edinburgh, Edinburgh EH16 4UU, U.K.

**Susan J. Rosser** – School of Biological Sciences, University of Edinburgh, Edinburgh EH9 3DW, U.K.; Centre for Engineering Biology, University of Edinburgh, Edinburgh EH9 3BF, U.K.; [orcid.org/0000-0002-2560-6485](https://orcid.org/0000-0002-2560-6485)

**Simon G. J. Mochrie** – Department of Physics, Yale University, New Haven, Connecticut 06520, United States; Integrated Graduate Program in Physical and Engineering Biology, Yale University, New Haven, Connecticut 06520, United States

**Marc Vendrell** – IRR Chemistry Hub, Institute for Regeneration and Repair and Centre for Inflammation Research, The University of Edinburgh, Edinburgh EH16 4UU, U.K.

Complete contact information is available at:  
<https://pubs.acs.org/10.1021/acs.nanolett.3c03780>

### Author Contributions

C.O., Z.G., E.J.J., Z.K., M.V., M.H.H., and L.R. designed experiments. Z.K., L.M.T., and F.d.M. synthesized labeled peptides and performed experiments to determine the binding kinetics of the peptides. AiryScan imaging and cell growth experiments were carried out by E.J.J. LIVE-PAINT yeast strains were generated by C.O. Z.G. performed all other experiments. Z.G., C.O., M.H.H., Z.K., H.B., E.J., S.J.R., S.G.J.M., and L.R. analyzed data. The manuscript was written by Z.G., C.O., M.H.H., and L.R., with contributions from all authors. All authors have given approval to the final version of the manuscript.

### Author Contributions

□ Z.G. and C.O. contributed equally to this work

### Funding

The authors acknowledge support from NIH R01 GM118528. Z.G. and Z.K. were funded via the BBSRC EastBIO doctoral training program (BB/M010996/1). C.O. was supported by the Yale Integrated Graduate Program in Physical and Engineering Biology. H.B. acknowledges the support of the Wellcome Trust via the Integrative Cell Mechanisms Ph.D. program (Grant Number 226437/Z/22/Z). The super-resolution instrument was funded by Dr Jim Love, UCB Pharma and the U.K. Dementia Research Institute.

### Notes

The authors declare no competing financial interest.

## ACKNOWLEDGMENTS

Confocal microscopy imaging was performed with Dr Toni McHugh at Centre Optical Instrumentation Laboratory (COL), which is supported by a Core Grant (203149) to the Wellcome Centre for Cell Biology at the University of Edinburgh. The knock-out yeast strains used in this study were kindly provided by the Edinburgh Genome Foundry. We would also like to thank Dr. Katherine Paine, Dr. Ella Thornton, Dr. Raef Shams, Dr. Mai-Britt Jensen, Dr. Rossana Boni, Noelia Pelegrina-Hidalgo, Kasia Stafaniak, and Sneha Ravi, for thoughtful comments on the manuscript.



## ABBREVIATIONS

FP, fluorescent protein; GFP, green fluorescent protein; SR, super-resolution; STED, stimulated emission depletion; RESOLFT, reversible saturable optical fluorescence transition; SIM, structured illumination microscopy; SMLM, single-molecule localization microscopy; PALM, photoactivation localization microscopy; PAINT, point accumulation for imaging in nanoscale topography; dSTORM, direct stochastic optical reconstruction microscopy; LIVE-PAINT, live cell imaging using reversible interactions point accumulation for imaging in nanoscale topography; mNG, mNeonGreen; TIRF, total internal reflection fluorescence; DL, diffraction-limited

## REFERENCES

- (1) Agbulut, O.; Coirault, C.; Niederländer, N.; Huet, A.; Vicart, P.; Hagege, A.; Puceat, M.; Menasché, P. GFP Expression in Muscle Cells Impairs Actin-Myosin Interactions: Implications for Cell Therapy. *Nat. Methods* **2006**, *3* (5), 331–331.
- (2) Lisenbee, C. S.; Karnik, S. K.; Trelease, R. N. Overexpression and Mislocalization of a Tail-Anchored GFP Redefines the Identity of Peroxisomal ER. *Traffic* **2003**, *4* (7), 491–501.
- (3) Hinrichsen, M.; Lenz, M.; Edwards, J. M.; Miller, O. K.; Mochrie, S. G. J.; Swain, P. S.; Schwarz-Linek, U.; Regan, L. A New Method for Post-Translationally Labeling Proteins in Live Cells for Fluorescence Imaging and Tracking. *Protein Eng. Des. Sel. PEDS* **2017**, *30* (12), 771–780.
- (4) Huh, W.-K.; Falvo, J. V.; Gerke, L. C.; Carroll, A. S.; Howson, R. W.; Weissman, J. S.; O'Shea, E. K. Global Analysis of Protein Localization in Budding Yeast. *Nature* **2003**, *425* (6959), 686–691.
- (5) Mason, A. B.; Allen, K. E.; Slayman, C. W. C-Terminal Truncations of the Saccharomyces Cerevisiae PMA1 H<sup>+</sup>-ATPase Have Major Impacts on Protein Conformation, Trafficking, Quality Control, and Function. *Eukaryot. Cell* **2014**, *13* (1), 43–52.
- (6) Rao, R.; Drummond-Barbosa, D.; Slayman, C. W. Transcriptional Regulation by Glucose of the Yeast PMA1 Gene Encoding the Plasma Membrane H<sup>+</sup>-ATPase. *Yeast* **1993**, *9* (10), 1075–1084.
- (7) Serrano, R. Characterization of the Plasma Membrane ATPase of Saccharomyces Cerevisiae. *Mol. Cell. Biochem.* **1978**, *22* (1), 51–63.
- (8) Szopinska, A.; Degand, H.; Hochstenbach, J.-F.; Nader, J.; Morsomme, P. Rapid Response of the Yeast Plasma Membrane Proteome to Salt Stress. *Mol. Cell. Proteomics MCP* **2011**, *10* (11), M111.009589.
- (9) Paine, K. M.; Ecclestone, G. B.; MacDonald, C. Fur4-Mediated Uracil-Scavenging to Screen for Surface Protein Regulators. *Traffic* **2021**, *22* (11), 397–408.
- (10) Betzig, E.; Patterson, G. H.; Sougrat, R.; Lindwasser, O. W.; Olenych, S.; Bonifacino, J. S.; Davidson, M. W.; Lippincott-Schwartz, J.; Hess, H. F. Imaging Intracellular Fluorescent Proteins at Nanometer Resolution. *Science* **2006**, *313* (5793), 1642–1645.
- (11) Hell, S. W.; Wichmann, J. Breaking the Diffraction Resolution Limit by Stimulated Emission: Stimulated-Emission-Depletion Fluorescence Microscopy. *Opt. Lett.* **1994**, *19* (11), 780–782.
- (12) Rust, M. J.; Bates, M.; Zhuang, X. Sub-Diffraction-Limit Imaging by Stochastic Optical Reconstruction Microscopy (STORM). *Nat. Methods* **2006**, *3* (10), 793–796.
- (13) Horrocks, M. H.; Palayret, M.; Klenerman, D.; Lee, S. F. The Changing Point-Spread Function: Single-Molecule-Based Super-Resolution Imaging. *Histochem. Cell Biol.* **2014**, *141* (6), 577–585.
- (14) Hofmann, M.; Eggeling, C.; Jakobs, S.; Hell, S. W. Breaking the Diffraction Barrier in Fluorescence Microscopy at Low Light Intensities by Using Reversibly Photoswitchable Proteins. *Proc. Natl. Acad. Sci. U. S. A.* **2005**, *102* (49), 17565–17569.
- (15) Heintzmann, R.; Cremer, C. G. Laterally Modulated Excitation Microscopy: Improvement of Resolution by Using a Diffraction Grating. *SPIE Proc.* **1999**, *3568*, 185–196.
- (16) Godin, A. G.; Lounis, B.; Cognet, L. Super-Resolution Microscopy Approaches for Live Cell Imaging. *Biophys. J.* **2014**, *107* (8), 1777–1784.
- (17) Gustafsson, M. G. Surpassing the Lateral Resolution Limit by a Factor of Two Using Structured Illumination Microscopy. *J. Microsc.* **2000**, *198* (2), 82–87.
- (18) Los, G. V.; Encell, L. P.; McDougall, M. G.; Hartzell, D. D.; Karassina, N.; Zimprich, C.; Wood, M. G.; Learish, R.; Ohana, R. F.; Urb, M.; Simpson, D.; Mendez, J.; Zimmerman, K.; Otto, P.; Vidugiris, G.; Zhu, J.; Darzins, A.; Klauert, D. H.; Bulleit, R. F.; Wood, K. V. HaloTag: A Novel Protein Labeling Technology for Cell Imaging and Protein Analysis. *ACS Chem. Biol.* **2008**, *3* (6), 373–382.
- (19) Keppler, A.; Gendreizig, S.; Gronemeyer, T.; Pick, H.; Vogel, H.; Johnsson, K. A General Method for the Covalent Labeling of Fusion Proteins with Small Molecules in Vivo. *Nat. Biotechnol.* **2003**, *21* (1), 86–89.
- (20) Gautier, A.; Juillerat, A.; Heinis, C.; Corrêa, I. R.; Kindermann, M.; Beauflis, F.; Johnsson, K. An Engineered Protein Tag for Multiprotein Labeling in Living Cells. *Chem. Biol.* **2008**, *15* (2), 128–136.
- (21) Pellett, P. A.; Sun, X.; Gould, T. J.; Rothman, J. E.; Xu, M.-Q.; Corrêa, I. R.; Bewersdorf, J. Two-Color STED Microscopy in Living Cells. *Biomed. Opt. Express* **2011**, *2* (8), 2364–2371.
- (22) Bottanelli, F.; Kromann, E. B.; Allgeyer, E. S.; Erdmann, R. S.; Wood Baguley, S.; Sirinakakis, G.; Schepartz, A.; Baddeley, D.; Toomre, D. K.; Rothman, J. E.; Bewersdorf, J. Two-Colour Live-Cell Nanoscale Imaging of Intracellular Targets. *Nat. Commun.* **2016**, *7* (1), 10778.
- (23) Bottanelli, F.; Kilian, N.; Ernst, A. M.; Rivera-Molina, F.; Schroeder, L. K.; Kromann, E. B.; Lessard, M. D.; Erdmann, R. S.; Schepartz, A.; Baddeley, D.; Bewersdorf, J.; Toomre, D.; Rothman, J. E. A Novel Physiological Role for ARF1 in the Formation of Bidirectional Tubules from the Golgi. *Mol. Biol. Cell* **2017**, *28* (12), 1676–1687.
- (24) Wilmes, S.; Staufenbiel, M.; Liße, D.; Richter, C. P.; Beutel, O.; Busch, K. B.; Hess, S. T.; Piehler, J. Triple-Color Super-Resolution Imaging of Live Cells: Resolving Submicroscopic Receptor Organization in the Plasma Membrane. *Angew. Chem., Int. Ed.* **2012**, *51* (20), 4868–4871.
- (25) Tas, R. P.; Albertazzi, L.; Voets, I. K. Small Peptide-Protein Interaction Pair for Genetically Encoded, Fixation Compatible Peptide-PAINT. *Nano Lett.* **2021**, *21* (22), 9509–9516.
- (26) Maity, B. K.; Nall, D.; Lee, Y.; Selvin, P. R. Peptide-PAINT Using a Transfected-Docker Enables Live- and Fixed-Cell Super-Resolution Imaging. *Small Methods* **2023**, *7* (4), 2201181.
- (27) Fischer, L. S.; Schlichthaerle, T.; Chrostek-Grashoff, A.; Grashoff, C. Peptide-PAINT Enables Investigation of Endogenous Talin with Molecular Scale Resolution in Cells and Tissues. *ChemBioChem.* **2021**, *22* (19), 2872–2879.
- (28) Oi, C.; Gidden, Z.; Holyoake, L.; Kantelberg, O.; Mochrie, S.; Horrocks, M. H.; Regan, L. LIVE-PAINT Allows Super-Resolution Microscopy inside Living Cells Using Reversible Peptide-Protein Interactions. *Commun. Biol.* **2020**, *3* (1), 1–10.
- (29) Yano, Y.; Yano, A.; Oishi, S.; Sugimoto, Y.; Tsujimoto, G.; Fujii, N.; Matsuzaki, K. Coiled-Coil Tag-Probe System for Quick Labeling of Membrane Receptors in Living Cells. *ACS Chem. Biol.* **2008**, *3* (6), 341–345.
- (30) Möller, S.; Croning, M. D. R.; Apweiler, R. Evaluation of Methods for the Prediction of Membrane Spanning Regions. *Bioinformatics* **2001**, *17* (7), 646–653.
- (31) Chen, R.; Rishi, H. S.; Potapov, V.; Yamada, M. R.; Yeh, V. J.; Chow, T.; Cheung, C. L.; Jones, A. T.; Johnson, T. D.; Keating, A. E.; DeLoache, W. C.; Dueber, J. E. A Barcoding Strategy Enabling Higher-Throughput Library Screening by Microscopy. *ACS Synth. Biol.* **2015**, *4* (11), 1205–1216.
- (32) Malinská, K.; Malinský, J.; Opekarová, M.; Tanner, W. Visualization of Protein Compartmentation within the Plasma Membrane of Living Yeast Cells. *Mol. Biol. Cell* **2003**, *14* (11), 4427–4436.

- (33) Gianni, S.; Engström, Å.; Larsson, M.; Calosci, N.; Malatesta, F.; Eklund, L.; Ngang, C. C.; Travaglini-Allocatelli, C.; Jemth, P. The Kinetics of PDZ Domain-Ligand Interactions and Implications for the Binding Mechanism\*. *J. Biol. Chem.* **2005**, *280* (41), 34805–34812.
- (34) Clowsley, A. H.; Kaufhold, W. T.; Lutz, T.; Meletiou, A.; Di Michele, L.; Soeller, C. Repeat DNA-PAINT Suppresses Background and Non-Specific Signals in Optical Nanoscopy. *Nat. Commun.* **2021**, *12* (1), 501.
- (35) Schaerer-Brodbeck, C.; Riezman, H. Saccharomyces Cerevisiae Arc35p Works through Two Genetically Separable Calmodulin Functions to Regulate the Actin and Tubulin Cytoskeletons. *J. Cell Sci.* **2000**, *113* (3), 521–532.
- (36) Ziółkowska, N. E.; Karotki, L.; Rehman, M.; Huiskonen, J. T.; Walther, T. C. Eisosome-Driven Plasma Membrane Organization Is Mediated by BAR Domains. *Nat. Struct. Mol. Biol.* **2011**, *18* (7), 854–856.
- (37) Brach, T.; Specht, T.; Kaksonen, M. Reassessment of the Role of Plasma Membrane Domains in the Regulation of Vesicular Traffic in Yeast. *J. Cell Sci.* **2011**, *124* (3), 328–337.
- (38) Montecinos-Franjola, F.; Bauer, B. L.; Mears, J. A.; Ramachandran, R. GFP Fluorescence Tagging Alters Dynamin-Related Protein 1 Oligomerization Dynamics and Creates Disassembly-Refractory Puncta to Mediate Mitochondrial Fission. *Sci. Rep.* **2020**, *10* (1), 14777.
- (39) Meyer, T.; Begitt, A.; Vinkemeier, U. Green Fluorescent Protein-Tagging Reduces the Nucleocytoplasmic Shuttling Specifically of Unphosphorylated STAT1. *FEBS J.* **2007**, *274* (3), 815–826.
- (40) Molle, J.; Raab, M.; Holzmeister, S.; Schmitt-Monreal, D.; Grohmann, D.; He, Z.; Tinnefeld, P. Superresolution Microscopy with Transient Binding. *Curr. Opin. Biotechnol.* **2016**, *39*, 8–16.
- (41) Bhaskar, H.; Kleinjan, D.-J.; Oi, C.; Gidden, Z.; Rosser, S. J.; Horrocks, M. H.; Regan, L. Live-Cell Super-Resolution Imaging of Actin Using LifeAct-14 with a PAINT-Based Approach. *Protein Sci.* **2023**, *32* (2), No. e4558.
- (42) Eklund, A. S.; Jungmann, R. Optimized Coiled-Coil Interactions for Multiplexed Peptide-PAINT. *Small* **2023**, *19* (12), 2206347.